

Theory of Resonant Optical Second-Harmonic Generation from a Focused Gaussian Beam*

R. ASBY†

Royal Holloway College, University of London, London, England

(Received 8 May 1969)

Optical second-harmonic generation (SHG) from a focused beam is studied using the methods and results developed in the previous paper. We consider specifically SHG from a Gaussian beam in a uniaxial medium such as lithium niobate, where phase matching is possible perpendicular to the optic axis, so that it is possible to neglect double refraction. An analytic expression for the single-harmonic output is given for the limiting cases: (a) when the nonlinear medium lies in the near fields of both the single-harmonic resonator and the Gaussian fundamental beam; (b) when the nonlinear medium lies in the far field of both these. For the general case, numerically computed curves are given for the dependence of the output on phase matching, focus position, and focusing. The optimum value of the focusing parameter l/z_0 (where l is the length of the nonlinear crystal and z_0 is $\frac{1}{2}$ the confocal parameter of the fundamental beam) for conversion into the Gaussian single-harmonic mode is $l/z_0 = 5.65$.

1. INTRODUCTION

THE problem of resonant second-harmonic generation (SHG) in the small-conversion approximation has been treated by Ashkin, Boyd, and Dziedzic¹ (ABD) and by Boyd and Kleinman² (BK) using plane-wave theory and the concept of coupling coefficients due to Kogelnik.³ We show in this paper how this problem becomes more transparent and much simpler using the coupled-mode formalism developed in the previous paper,⁴ hereafter referred to as I. This problem is the simplest to which this formalism may be applied, since in the small-conversion approximation there is no reaction back on the fundamental and hence only its original Gaussian mode need be considered.

We consider a traveling-wave Gaussian beam

$$E_1(x, y, z) = \frac{A}{w_{01}} \left(\frac{2}{\pi} \right)^{1/2} \frac{1}{1 - i\xi_1} \times \exp\left(-\frac{x^2 + y^2}{w_{01}^2(1 - i\xi_1)} - ik_1 z \right), \quad (1.1)$$

where $\xi_1 = 2z/k_1 w_{01}^2 = z/z_0$, and z_0 is $\frac{1}{2}$ the confocal parameter of the fundamental beam in the medium. This beam impinges on an open resonator containing uniaxial nonlinear dielectric orientated with its optic axis perpendicular to the axis of the resonator (Fig. 1).

As before, lithium niobate is taken as the nonlinear dielectric. The phase-matching condition can then be satisfied and can be controlled by means of the crystal temperature.⁵

* Research supported in part by the Ministry of Technology (Great Britain), under Contract No. PD/89/04/AT, and by the U. S. Army Research Office (Durham).

† Present address: Department of Physics and Astronomy, University of Rochester, Rochester, N. Y. 14627.

¹ A. Ashkin, G. D. Boyd, and J. M. Dziedzic, *J. Quantum Electron.* **QE2**, 109 (1966).

² G. D. Boyd and D. A. Kleinman, *J. Appl. Phys.* **39**, 3597 (1968).

³ H. Kogelnik, in *Proceedings of the Symposium on Quasi-Optics, New York, 1964* (Polytechnic Press, Brooklyn, N. Y., 1964), p. 333.

⁴ R. Asby, preceding paper, *Phys. Rev.* **187**, 1062 (1969).

⁵ G. D. Boyd, R. C. Miller, K. Nassau, W. L. Bond, and A. Savage, *Appl. Phys. Letters* **5**, 234 (1964).

To avoid reflection and refraction at the surfaces of the nonlinear dielectric it is assumed to be imbedded in a material of the same refractive index. It is also assumed that the mirrors of the resonator are transparent to the fundamental beam and that the alignment of this beam to the cavity is perfect. The theory may be extended to cover the case of imperfect alignment as indicated in I.

In the small-conversion approximation the problem splits into two parts. First, there is the calculation of the increase in the various second-harmonic mode amplitudes produced by a single pass of the dielectric. This calculation is also relevant to the case of "free" (i.e., in the absence of the second-harmonic resonator) SHG, where the second-harmonic beam parameters are determined directly by the fundamental beam parameters. In the resonant case these parameters are determined by the cavity. The second calculation is the determination of the mode amplitudes in the resonator and hence the output using the previous results and the loss parameters of the resonator. This part follows exactly the method of ABD and BK. Absorption in the nonlinear media will be neglected in the calculation of the single-pass outputs since its inclusion produces no new effects except that an optimum crystal length can then be defined which depends on the amount of absorption present at each frequency.² All absorption is included in the calculation of the resonator output as part of the resonator losses.

From I, we see that the mode functions of the second-

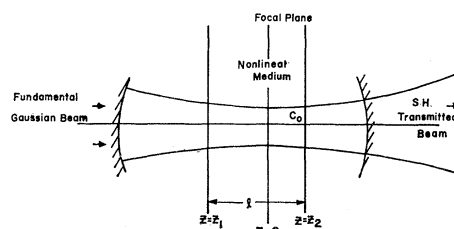


FIG. 1. Second-harmonic resonator cavity.

harmonic cavity are given by

$$E_{nm} = \frac{\sqrt{2}B_{nm}}{w_{02}\bar{e}^{1/2}(2^{n+m}n!m!)^{1/2}} \times \frac{(1+i\xi_2)^{(n+m)/2}}{(1-i\xi_2)^{(n+m)/2+1}} H_n\left(\frac{\bar{e}x\sqrt{2}}{w_{02}}\right) H_m\left(\frac{y\sqrt{2}}{w_{02}}\right) \times \exp\left(-\frac{\bar{e}^2x^2+y^2}{w_{02}^2(1-i\xi)} - ik_2z\right), \quad (1.2)$$

where $\bar{e} = (\epsilon_z/\epsilon_x)^{1/2}$.

$$C_{nm} = \frac{-4\sqrt{2}\pi^{1/2}i\omega^2d_{31}\bar{e}^{1/2}(2n!2m!)^{1/2}e^{i\Delta kz}}{k_2c^2w_{02}n!m!2^{n+m}} \frac{[\bar{e}^2w^2-1-i(\bar{e}^2w^2\xi_1-\xi_2)]^n[w^2-1-i(w^2\xi_1-\xi_2)]^m}{[\bar{e}^2w^2+1-i(\bar{e}^2w^2\xi_1-\xi_2)]^{n+1/2}[w^2+1-i(w^2\xi_1-\xi_2)]^{m+1/2}}, \quad (1.4)$$

where $\Delta k = k_2 - 2k_1$, $w = w_{01}/\sqrt{2}w_{02}$. The expression for the coupling coefficient may be simplified by noting that for $\Delta k \ll k_1k_2$, we have

$$w^2\xi_1 - \xi_2 = 0 \quad (1.5)$$

and

$$\bar{e}^2w^2\xi_1 - \xi_2 = -\bar{e}^2w^2\xi_1\epsilon,$$

where $\epsilon = -(1-1/\bar{e}^2)$. Thus C_{nm} becomes

$$C_{nm} = \frac{\alpha_{nm}\bar{e}^{1/2}(\bar{e}^2w^2-1+i\bar{e}^2w^2\xi_1\epsilon)^n(w^2-1)^m e^{i\Delta kz}}{w_{02}(1-i\xi)(\bar{e}^2w^2+1+i\bar{e}^2w^2\xi_1\epsilon)^{n+1/2}(w^2+1)^{m+1/2}}, \quad (1.6)$$

where α_{nm} represents the normalizing coefficients.

In the small-conversion approximation the fundamental mode amplitude is assumed constant; hence

$$B_{nm}(z_2) = A^2 \int_{z_1}^{z_2} C_{nm} dz, \quad (1.7)$$

where $z = z_1$, z_2 are the boundaries of the nonlinear dielectric. The physical length of the dielectric is thus $l = z_1 - z_2$.

2. NEAR-FIELD WEAK-FOCUSING LIMIT

This is the case treated by ABD when the nonlinear dielectric lies within the near field of both the second-harmonic and the fundamental beams, i.e., where both $\xi_1 \ll 1$ and $\xi_2 \ll 1$. By this method, two important aspects of the problem are brought out immediately; first, the variation of the coupling coefficients with the relative spot sizes of the two beams; second, the new phase-matching condition.

A. Lowest-Order Coupling C_{00}

To the first order in ξ_1 , we may approximate

$$(\bar{e}^2w^2+1+i\bar{e}^2w^2\epsilon\xi_1)^{-1/2} = (\bar{e}^2w^2+1)^{-1/2} \exp\left(\frac{-i\bar{e}^2w^2\epsilon\xi_1}{2(\bar{e}^2w^2+1)}\right). \quad (2.1)$$

Using this approximation, we have from Eq. (1.6)

The rate of change of the $2n2m$ th second-harmonic mode amplitude $B_{2n,2m}$ in the nonlinear medium is given by Eq. (5.13) of I:

$$dB_{nm}/dz = C_{nm}A^2, \quad (1.3)$$

where, since by symmetry only even modes will be generated, the notation has been simplified by replacing $2n2m$ by nm . The fundamental mode parameters have also been omitted since only one mode of the fundamental beam is being considered. The coupling coefficient C_{nm} is given by the equation

and (1.7)

$$B_{00}(z_2) = \frac{\alpha_{00}A^2}{\bar{e}^{1/2}w_{02}(\bar{e}^2w^2+1)^{1/2}(w^2+1)^{1/2}} \times \int_{z_1}^{z_2} \exp\left(i\Delta kz + i\xi_1 - \frac{i\bar{e}^2w^2\epsilon\xi_1}{2(\bar{e}^2w^2+1)}\right) dz. \quad (2.2)$$

Thus the variation of the output in the lowest-order mode with spot size is given to a good approximation by the function

$$F(w_{01}, w_{02}) = \bar{e}^{1/2}/w_{02}(\bar{e}^2w^2+1)^{1/2}(w^2+1)^{1/2}. \quad (2.3)$$

For constant w_{02} , this function increases with decreasing w (i.e., decreasing w_{01}). Since the resonator mode functions are only valid for $w_{01} \gg \lambda$, this just implies that for maximum output the fundamental spot size w_{01} must be as small as possible, as would be expected. For constant w_{01} the variation of $F(w_{01}, w_{02})$ is shown in Fig. 2. The function has a maximum at $w = \bar{e}^{-1/2}$, which for $\bar{e}^2 = 0.96$ (an approximate value for lithium niobate) is equal to 1.01.

Substituting for $\xi_1 = 2z/k_1w_{01}^2$ in Eq. (2.2), the new phase-matching condition can be seen immediately to be

$$\Delta k = -(k_1w_{01}^2)^{-1}[1 - \bar{e}^2w^2\epsilon/2(\bar{e}^2w^2+1)]. \quad (2.4)$$

This has been referred to as the optimum phase-matching condition.⁶ When $w = 1.01$, this becomes

$$\Delta k = -0.99/k_1w_{01}^2. \quad (2.5)$$

⁶ D. A. Kleinman, A. Ashkin, and G. D. Boyd, Phys. Rev. 145, 338 (1966).

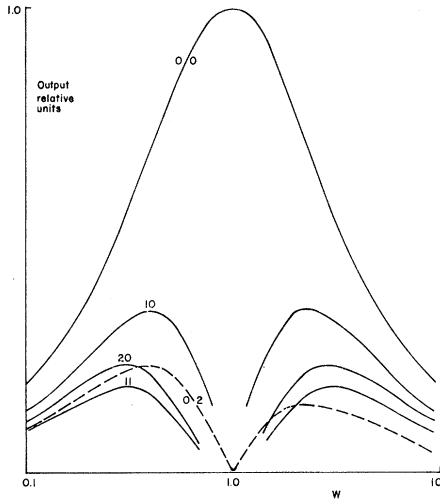


FIG. 2. Variations of the output amplitude of various modes of the second-harmonic with the relative spot size $w = w_{01}/\sqrt{2}w_{02}$.

In the plane-wave limit $w_{01} \rightarrow \infty$, this expression tends to the usual $\Delta k = 0$ as expected, but it can be substantially different from this limit for normal experimental spot sizes $\sim 10^{-2}$ cm.

B. Higher-Order Coefficients

When $\bar{\epsilon}w - 1$ is not near zero, the same approximation procedure as that used for the lowest-order coefficient may be used, and from this we obtain

$$C_{nm} = \frac{\alpha_{nm}(w^2 - 1)^m (\bar{\epsilon}^2 w^2 - 1)^n}{w_{02}(w^2 + 1)^{m+1/2} (\bar{\epsilon}^2 w^2 + 1)^{n+1/2}} \exp \left\{ i\Delta k z + i\xi_1 \right. \\ \left. \times \left[1 + \bar{\epsilon}^2 w^2 \epsilon \left(\frac{n}{\bar{\epsilon}^2 w^2 - 1} - \frac{2n+1}{2(e^2 w^2 + 1)} \right) \right] \right\}. \quad (2.6)$$

The spot size function

$$F_{nm}(w_{01}, w_{02}) = \frac{(w^2 - 1)^m (e^2 w^2 - 1)^n}{\bar{\epsilon}^{1/2} w_{02} (w^2 + 1)^{m+1/2} (\bar{\epsilon}^2 w^2 + 1)^{n+1/2}} \quad (2.7)$$

again has the property that when the second-harmonic spot size w_{02} is held constant, it increases with decreasing fundamental spot size w_{01} . When the fundamental spot size is held constant, the function has two distinct maxima which for $\bar{\epsilon} = 1$ occur at reciprocal points. The variation of a few of the lower-order functions is plotted in Fig. 2 for $\bar{\epsilon} = 0.98$. It can be seen that the value of w at which the maximum occurs increases with increasing mode number. This is shown by the similar function which occurs in the two-dimensional problem:

$$F_n(w_{01}, w_{02}) = (w^2 - 1)^n / w_{02}^{1/2} (w^2 + 1)^{n+1/2}, \quad (2.8)$$

for which

$$w_{\max} = 4n + 1 \pm [(4n + 1)^2 - 1]^{1/2}. \quad (2.9)$$

Phase matching for the nm th mode occurs when

$$\Delta k = -\frac{1}{k_1 w_{01}^2} \left[1 + \bar{\epsilon}^2 w^2 \left(\frac{n}{\bar{\epsilon}^2 w^2 - 1} - \frac{2n+1}{2(\bar{\epsilon}^2 w^2 + 1)} \right) \right]. \quad (2.10)$$

This expression depends on n , the xz -plane mode number, but not on the other mode number m . Thus it can be seen that by suitably adjusting the phase matching and the relative spot size to some extent, the output in a particular mode may be enhanced, although, in general, the output in the lowest-order mode will always be dominant.

If $|\bar{\epsilon}w - 1| \ll 1$, then all the coefficients except $C_{1,m}$ are of higher order in ξ_1 than the first and hence may be neglected in the near-field approximation. The $C_{1,m}$ are given by

$$C_{1,m} = \frac{\alpha_{1m}(w^2 - 1)^m i \bar{\epsilon}^2 w^2 \epsilon \xi_1}{w_{02}(w^2 + 1)^{m+1/2} (e^2 w^2 + 1)^{n+1/2}} \\ \times \exp \left\{ iz \left[\Delta k + \frac{1}{k_1 w_{01}^2} \left(1 - \frac{(2n+1)\bar{\epsilon}^2 w^2}{2(e^2 w^2 + 1)} \right) \right] \right\} \quad (2.11)$$

and are negligible compared with C_{00} , which has its maximum in this range of w .

3. FAR FIELD

The second limiting case which may be evaluated analytically is the case when the nonlinear dielectric lies in the far field of both the fundamental and second-harmonic beams. This case has little practical importance, but it is included for completeness. Under the far-field approximations $\xi_1 \gg 1$, $\xi_2 \gg 1$, C_{00} can be written

$$C_{00} = \frac{-\alpha_{00}}{w_{02}(w^2 + 1)^{1/2} w} \left(\frac{k_1^3 w_{01}^6}{-i\bar{\epsilon}^2 \epsilon z^3} \right)^{1/2} e^{i\Delta k z},$$

and hence the second-harmonic output from a slab of dielectric length $l = z_2 - z_1$ is proportional to

$$I = \int_{z_1}^{z_2} \frac{e^{i\Delta k z}}{z^{3/2}} dz,$$

which becomes, on the assumption that the thickness of the slab is much smaller than its distance from the focus of the beams $l/z \ll 1$,

$$I = \frac{e^{i\Delta k z_1}}{z_1^{3/2}} \int_0^l e^{i\Delta k z} dz,$$

to the first order. The phase-matching condition in this limit is just that which arises in the plane-wave case and the output varies with the usual $\sin(\frac{1}{2}\Delta k l) / \frac{1}{2}\Delta k l$.

4. INFINITE-CRYSTAL STEEP-FOCUSING LIMIT

In the limit of an infinitely thick slab of dielectric, or, equivalently, the steep-focusing limit, the expression

for the amplitude of the second-harmonic output in the lowest-order mode is given by

$$C_{00} = \frac{\alpha_{00}}{w_{02}(w^2+1)^{1/2}} \int_{-\infty}^{\infty} \frac{e^{i\Delta k z} dz}{(1-i\xi_1)(\bar{e}^2 w^2 + 1 + i\bar{e}^2 w^2 \epsilon \xi_1)^{1/2}}$$

Changing the variable of integration to $\xi = v$, the integral becomes

$$I = \int_{-\infty}^{\infty} \frac{e^{iyv} dv}{(1-iv)(a+ibv)^{1/2}},$$

where $y = \Delta k/k_1 w_{01}^2$, $a = e^2 w^2 + 1$, and $b = e^2 w^2 \epsilon$.

This integral may be evaluated under certain conditions by contour integration in the complex v plane. For $y < 0$, consider the integral around the contour made up from a semicircle radius R in the lower half-plane and the completing section of the real axis. In the limit $R \rightarrow \infty$ the integral around the semicircle tends to zero. The contour contains the simple pole at $v = -i$; hence from Cauchy's theorem

$$I = -2\pi ey / (a+b)^{1/2} \quad \text{for } y < 0.$$

The integral has a branch point on the upper half-plane at $v = ia$ and so cannot be integrated immediately for $y > 0$. However, since b is small, the limit $b \rightarrow 0$ will give an indication of the behavior of the integral. In this limit, the integrand is analytic in the upper half-plane, and hence, integrating around a contour completed in the upper half-plane, we have by Cauchy's theorem

$$I = 0 \quad \text{for } y > 0, b = 0.$$

Thus we expect the integral to exhibit something of a discontinuity at $y = 0$, i.e., $\Delta k = 0$. This general behavior can be seen in Fig. 7, which records the variation of the integral I with Δk for $l/z_0 = 100$. This shows clearly this asymptotic form. The integral in the limit $b = 0$ has been considered by Kleinman, Ashkin, and Boyd,⁶ in a different context. They obtain a continuous analytic approximation to it which shows the fine structure evident in Fig. 7.

5. GENERAL BEHAVIOR

A. Lowest-Order Mode

From Eqs. (1.6) and (1.7), the second-harmonic output in the lowest-order mode is given by the equation

$$C_{00} = \frac{\alpha_{00} w z_0}{w_{01}(w^2+1)^{1/2}} \int_{\xi_1}^{\xi_2} \frac{e^{i v \xi} d\xi}{(1-i\xi)(a+ib\xi)^{1/2}}, \quad (5.1)$$

where $z_0 = k_1 w_{01}^2$, $y = \Delta k z_0$, $a = \bar{e}^2 w^2 + 1$, and $b = e^2 w^2 \epsilon$. y contains the mismatch parameter, $\xi_1 = z_1/z_0$ and $\xi_2 = z_2/z_0$ contain the length of the nonlinear slab $l = (\xi_2 - \xi_1)z_0$, and the position of the focus of the two beams (assumed coincident) $f = \frac{1}{2}(\xi_1 + \xi_2)z_0$. The variation of the output with the focusing parameter z_0 , which is $\frac{1}{2}$ the confocal length of the associated resonator, can

be obtained by rearranging Eq. (5.1) in the form

$$C_{00} = \frac{\alpha_{00} w}{(w^2+1)^{1/2}} \frac{(\frac{1}{2} k_1 l)^{1/2}}{(\xi_2 - \xi_1)^{1/2}} \times \int_{\xi_1}^{\xi_2} \frac{e^{i v \xi} d\xi}{(1-i\xi)(a+ib\xi)^{1/2}} \quad (5.2)$$

and studying the variation of this form with ξ_1, ξ_2 for a given focus position f .

A computer program was developed which evaluated the integral using Simpson's rule. The results are shown in Figs. 2-13. Figures 3-7 show the second-harmonic output variation with the phase-matching parameter $\frac{1}{2} \Delta k l$ for various relative crystal lengths $\xi_l = l/z_0$, with the foci coincident, at the center of the crystal. Figure 3 shows the variation for the shortest crystal length $\xi_l = 0.4$. This curve shows clearly the near-field limit appearance. It has the form $\sin(x)/x$ with the absolute maximum slightly off $\Delta k = 0$. Away from phase match-

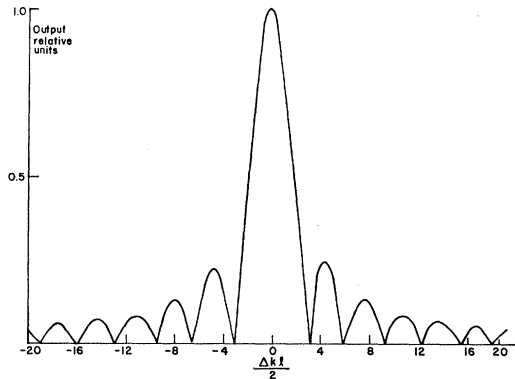


FIG. 3. Variation of the output amplitude in the second-harmonic Gaussian mode with phase matching for a relative crystal length $l/z_0 = 0.4$.

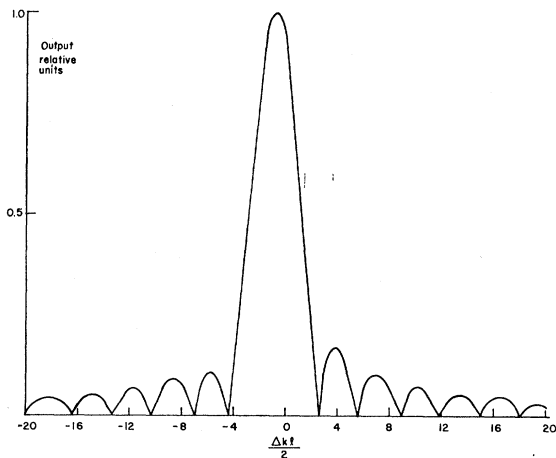


FIG. 4. Variation of the output amplitude in the second-harmonic Gaussian mode with phase matching for a relative crystal length $l/z_0 = 2.5$.

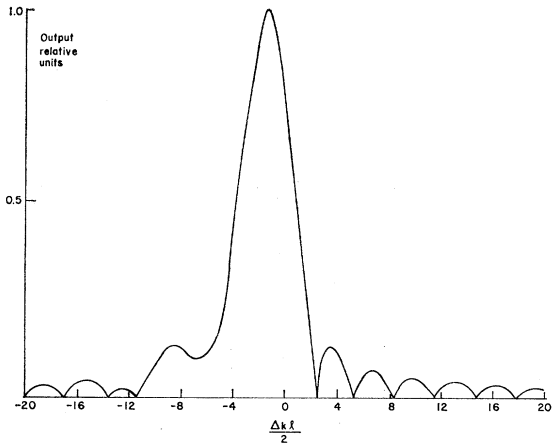


FIG. 5. Variation of the output amplitude in the second-harmonic Gaussian mode with phase matching for the optimum relative length $l/z_0=5.65$.

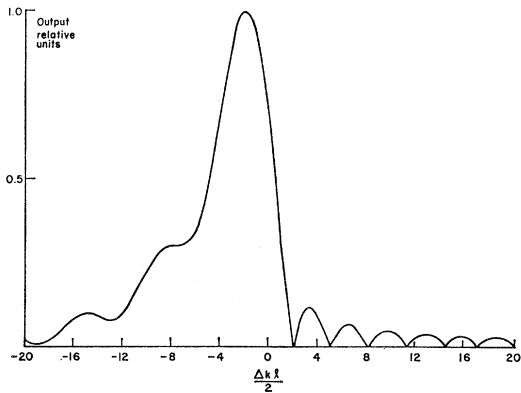


FIG. 6. Variation of the output amplitude in the second-harmonic Gaussian mode with phase matching for a relative crystal length $l/z_0=10$.

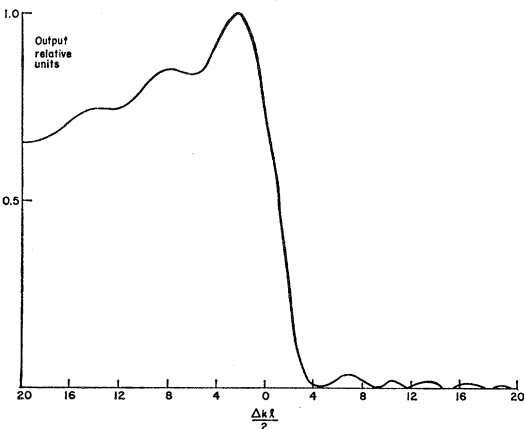


FIG. 7. Variation of the output amplitude in the second-harmonic Gaussian mode with phase matching for a relative crystal length $l/z_0=100$.

ing all the curves (Figs. 3-7) exhibit a periodicity of π , the familiar "coherence-length" effect (cf. the plane-wave interaction¹ proportional to $\sin \frac{1}{2} \Delta k l$).

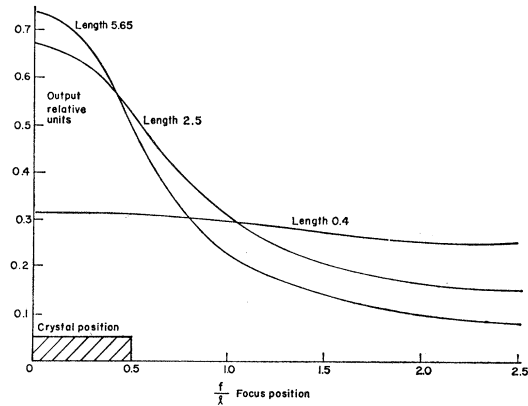


FIG. 8. Variation of second-harmonic output in the Gaussian mode at optimum phase matching with focus position relative to the crystal (the foci of the two beams assumed coincident).

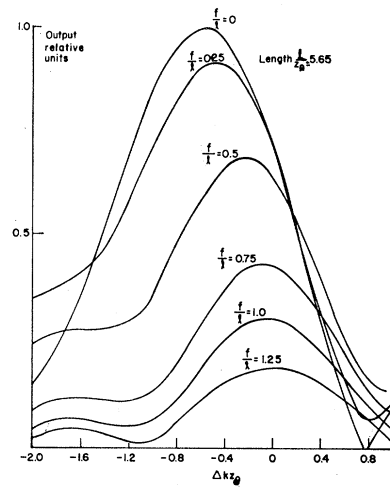


FIG. 9. Variation of the second-harmonic output amplitude in the Gaussian mode with phase matching for various positions of the focus.

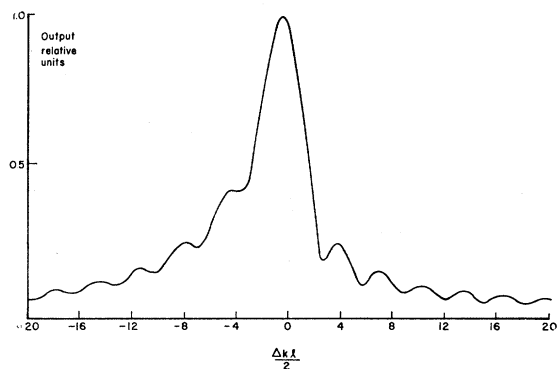


FIG. 10. Variation of the second-harmonic output amplitude in the Gaussian mode with phase matching with the focus at the face of the crystal.

As the length of the crystal increases or, equivalently, the focusing increases (z_0 decreases), the curves become asymmetric. The optimum phase-matching position

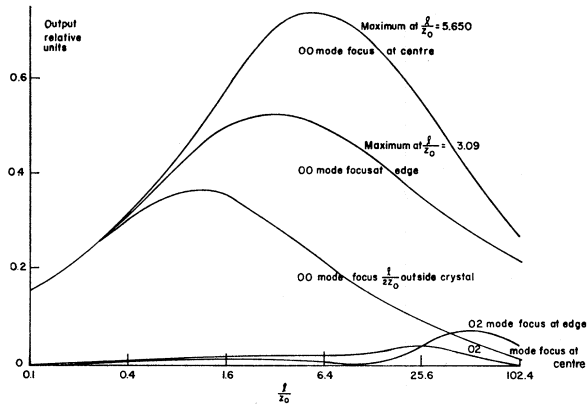


FIG. 11. Variation of the second-harmonic output in the first two modes with focusing for two positions of the focus.

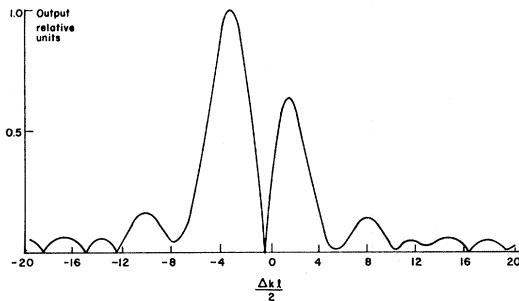


FIG. 12. Variation of the second-harmonic output in the 0-2 mode with phase-matching, with the focus at the center of the crystal.

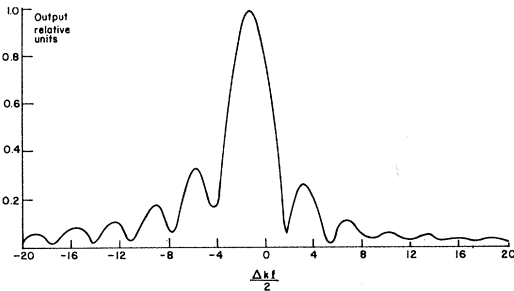


FIG. 13. Variation of the second-harmonic output in the 0-2 mode with phase matching, with the focus at the face of the crystal.

moves away from $\Delta k = 0$ and the central peak becomes wider on the side $\Delta k = 0$, engulfing the smaller peaks. This marks the increasing effect of the focusing terms in the denominator of the integrand of Eqs. (5.1) and (5.2).

If the Gaussian beams are considered as a sum of plane waves propagating over a range of directions, the reason for the asymmetry becomes apparent. When $\Delta k > 0$, the fundamental and second-harmonic refractive index ellipsoids do not intersect for any direction of propagation; hence none of the constituent plane waves is phase-matched. When $\Delta k < 0$, the index surfaces

intersect for some direction of propagation, and so there exist plane waves in the sum which are phase-matched. The steep-focusing infinite-crystal effect can be seen clearly in Fig. 9 as was previously pointed out. All these curves are consistent with those given by BK.

Figure 11 shows the variation of the output with focusing, at the optimum phase matching and optimum relative spot size for three positions of the focus. With the focus at the center of the crystal the maximum occurs at $l/z_0 = 5.65$, which may be compared with the result given by BK for "free" SHG of $l/z_0 = 5.68$. The slight difference between the two results may be explained as follows. If the second-harmonic generated in the absence of a resonator is regarded as being made up of a number of resonator modes, the higher modes will contribute a small amount to the total. The higher modes have their maximum output at a higher degree of focusing than the lowest-order Gaussian mode and hence the maximum output from the sum will occur at a higher degree of focusing than the maximum output for the lowest-order mode.

With the foci of the beams at the entry face or exit face of the crystal, the maximum occurs at $l/z_0 = 3.09$ as shown in the second curve of Fig. 11. This figure would of course be the optimum required if the second-harmonic resonator were planoconcave. The third curve represents the case when the focus is $\frac{1}{2}$ the crystal length outside the crystal. There the curve has an early maximum and falls off sharply as the focal region withdraws from the crystal. Also shown in Fig. 11 is the output in the 0-2 mode under this same conditions of phase matching and spot size as the corresponding curves for the Gaussian mode.

Figure 8 shows the variation of output with focus position for several relative crystal lengths at optimum phase matching and spot size. Figure 9 shows the variation of the shape of the output curve with phase-match angle as the foci move away from the center of the crystal. As expected from the consideration of the far-field limit, the optimum phase-match position moves toward $\Delta k = 0$ and the shape of the curve approaches

$$\sin(\frac{1}{2}\Delta kl) / \frac{1}{2}\Delta kl.$$

A greater range of Δk is shown on Fig. 10 for the case when the focus is at the face of the crystal. It can be seen that the minima have moved up from zero and the curve has taken on much of the form of the steep-focusing limit. These effects may be shown to be due to the increasing effect of the anisotropy of the medium by expanding the integrand in Eq. (4.1) in powers of $\epsilon = -(1 - \epsilon_x/\epsilon_z)$.

B. 0-2 Mode

When the various parameters have been adjusted for optimization of the second-harmonic output in the Gaussian mode, the 0-2 mode $n = 0$, $m = 1$ of the higher modes will contribute the most to the output. The

output in this mode is given from Eqs. (1.6) and (1.7) by

$$C_{01} = \frac{\alpha_{01}}{w_{02}} \int_{z_1}^{z_2} \frac{(\bar{\epsilon}^2 w^2 - 1 + i\bar{\epsilon}^2 w^2 \epsilon \xi_1) e^{i\Delta k z}}{(\bar{\epsilon}^2 w^2 + 1 + i\bar{\epsilon}^2 w^2 \epsilon \xi_1)^{3/2} (1 - i\xi_1)} dz.$$

The same computer program was used to evaluate this integral as was used for the Gaussian mode. Figures 12 and 13 show the output variation of this mode with phase matching for a crystal of length $l/z_0 = 5.65$, the optimum value for the Gaussian mode. With the foci of the beams at the center of the crystal (Fig. 12) the output exhibits a marked double peak which is present at all the crystal lengths. The relative heights of these peaks change with crystal length. As the focus moves away from the center (Fig. 13) the second peak decreases in height and the curve takes on the form of those of the Gaussian mode. The position of the twin peaks in Fig. 13 changes very little with varying crystal length; this gives rise to the dip in the curve for the 0-2 mode, foci at the center, in Fig. 11. Both curves for the Gaussian and 0-2 modes are drawn under the same phase-matching conditions, those which are optimum for the Gaussian mode. The dip occurs as the optimum phase-matching position for the Gaussian mode moves through the region between the twin peaks of Fig. 12.

Although the output variation with relative spot size for the Gaussian mode has the form indicated on Fig. 2 at the optimum length, the curve for the output in the 0-2 mode differs from that of the 2-0, and is shown dotted in Fig. 2.

When the Gaussian mode is optimized, the relative outputs for the two modes are

$$|C_{00}/C_{01}| \sim 100$$

when the foci are at the center of the crystal and

$$|C_{00}/C_{01}| \sim 50$$

when the foci are at the entry or exit face.

6. CALCULATION OF OUTPUT FROM RESONANT CAVITY

The calculation of the output of the cavity follows the method given by ABD. Referring to Fig. 1, C_0 is defined as the amplitude of the relevant mode just inside the crystal exit face, and $re^{i\phi}$ is the power loss parameter of the cavity. This parameter includes all losses, diffraction, reflection, absorption, and the loss due to the output. In the absence of SHG after a single round trip the mode amplitude would thus be

$$C = C_0 r e^{i\phi}. \quad (6.1)$$

Since the second-harmonic power is only generated as the wave travels from left to right, the amplitude in the

presence of SHG is given by the equation

$$C_0 = C_0 r e^{i\phi} + C_1, \quad (6.2)$$

where C_1 is the second-harmonic generated in a single pass, the quantity which has been discussed in the previous sections.

Rearranging Eq. (6.2), we have

$$C_0 = C_1 / (1 - r e^{i\phi}), \quad (6.3)$$

and thus the power output of the resonator is given by

$$P = t |C_1|^2 / (1 - 2r \cos\phi + r^2), \quad (6.4)$$

where t is the transmission coefficient of the output mirror. As pointed out by ABD, this output P can be much greater than the single-pass output $|C_1|^2$, and hence the second-harmonic conversion can be much enhanced by the resonator.

The tuning of the resonator through the parameter ϕ can be used to discriminate against unwanted modes, since the modes resonate at slightly different frequencies. When the resonator is tuned for optimum output in the lowest-order Gaussian mode, the output in the 0-2 mode can be as small as 10^{-4} of that in the Gaussian mode. This ratio of course depends on the resonator parameters.

7. CONCLUSION

In this paper, we have discussed the theory of resonant SHG from a Gaussian beam using the methods and results of I. Resonant SHG from a Gaussian beam is the simplest situation to which this theory can be applied. We have shown that the results are consistent with those given by previous authors using a different method.

We have examined in detail only the output into the lowest-order mode. The theory applies without modification to any higher-order mode. Thus the contribution from each mode to the total output can be determined for any value of the various resonator parameters. The first sections of the paper also apply to "free" SHG (i.e., in the absence of a second-harmonic resonator), when the parameters of the second-harmonic modes will be determined by those of the fundamental.

The theory can be extended using the results of I to SHG in the low-conversion approximation from any given mode and hence from a sum of modes, and also to the case of sum and difference frequency mixing in the low-conversion approximation.

ACKNOWLEDGMENTS

I acknowledge with pleasure the help and encouragement given by Dr. E. H. Hutten and the many helpful discussions with Dr. M. J. Colles and Dr. R. C. Smith of Southampton University.